KeAi

Engineered Regeneration

Volume 5 • Issue 3 • September 2024

ScienceDirect

Engineered Regeneration

Q1

Biomaterials

best quartile

SJR 2023

2.97

Editorial Board

Open access ISSN: 2666-1381

Editors-in-Chief

Yuanjin Zhao
Department of Clinical Laboratory, The Affiliated Drum Tower Hospital of Nanjing University Medical School, Nanjing, China

Email Yuanjin Zhao

Donghui Zhu
Department of Biomedical Engineering, Stony Brook University, Stony Brook, NY, United States

Email Donghui Zhu

Associate Editors

Anna Blocki
Institute for Tissue Engineering and Regenerative Medicine, The Chinese University of Hong Kong, Hong Kong, China

Bin Duan
University of Nebraska Medical Center, Omaha, NE, United States

Amir M Ghaemmaghami
Faculty of Medicine & Health Sciences, University of Nottingham, Nottingham, UK

Kee Woei Ng
School of Materials Science & Engineering, Nanyang Technological University, Singapore,

i3S - Instituto de Investigação e Inovação em Saúde, Universidade do Porto, Porto, Portugal

Malcolm Xing
Department of Mechanical Engineering, University of Manitoba, Manitoba, Canada

Hongbo Zhang
Pharmaceutical Sciences Laboratory and Turku Bioscience Centre, Abo Akademi University, Turku, Finland

Qiang Zhao
State key Laboratory of Medicinal Chemical Biology, College of Life Sciences, Nankai University, Tianjin, China

Editorial Board Members

Liming Bian
Biomaterials and Regenerative Medicine, South China University of Technology, Guangdong, China

Gulden Camci-Unal
Department of Chemical Engineering, University of Massachusetts Lowell, Lowell, MA, USA

Xanthippi Chatzistavrou
Chemical Engineering and Materials Science, Michigan State University, East Lansing, MI, United States

Zetao Chen
Hospital of Stomatology, Sun Yat-sen University, Guangzhou, China

Ke Cheng
Department of Biomedical Engineering, Columbia University, NY, United States

Wenguo Cui
Shanghai Key Laboratory for Prevention and Treatment of Bone and Joint Diseases, Shanghai Institute of Traumatology and Orthopaedics, Ruijin Hospital, Shanghai Jiao Tong University School of Medicine, Shanghai, China

Scott H. Medina
Department of Biomedical Engineering, The Pennsylvania State University, University Park, PA, United States

Caiwen Qu
Department of Cardiology, the Zhujiang Hospital of Southern Medical University, Guangzhou, China

Guoqing Pan
Institute for Advanced Materials, School of Materials Science and Engineering, Jiangsu University, Zhenjiang, China

Fuzeng Ren
Department of Materials Science and Engineering, Southern University of Science and Technology, Shenzhen, China

Ling Ren
Institute of Metal Research, Chinese Academy of Sciences, Shenyang, China

Jessica Rosenholm
Pharmaceutical Sciences Laboratory, Faculty of Science and Engineering, ˚bo Akademi University, Turku, Finland

Hélder A. Santos
Division of Pharmaceutical Chemistry and Technology, Helsinki One Health (HOH), University of Helsinki, Helsinki, Finland

Jinwei Tian
The Second Affiliated Hospital of Harbin Medical University, Harbin, China

Chunming Wang
Institute of Chinese Medical Sciences, University of Macau, Macau, China

Huaiyu Wang
Shenzhen Institute of Adcanced Technology, Chinese Academy of Sciences, Shenzhen, China

Shuqi Wang
1. State Key Laboratory for Diagnosis and Treatment of Infectious Diseases, National Clinical Research Center for Infectious Diseases, Collaborative Innovation Center for Diagnosis and Treatment of Infectious Diseases, The First Affiliated Hospital, College of Medicine, Zhejiang University, Hangzhou, China
2. Institute for Translational Medicine, Zhejiang University, Hangzhou, China

Jin Zhou
Department of Neural Engineering and Biological Interdisciplinary Studies, Institute of Military Cognition and Brain Sciences, Academy of Military Medical Sciences, Beijing, China

Submit your paper

View articles

Guide for Authors

Abstracting and Indexing

Recent Articles

Most Downloaded Articles

News

Most Cited Articles

Call for Papers

Featured Papers

ScienceDirect

Engineered Regeneration

Open access

22.9
CiteScore

Volume 5, Issue 3

Pages 283-432 (September 2024)

Download full issue

Previous vol/issue Next vol/issue

Review

Advances in nano silver-based biomaterials and their biomedical applications

Punuri Jayasekhar Babu, Akriti Tirkey, Abraham Abbey Paul, Kathelina Kristollari, ... Robert S. Marks
Pages 326-341

View PDF Article preview

Review article *Open access*

Instability-Driven 3D bioprinting for engineering composite bio-inks

Jing Ma, Cheng Qi, Zhou Liu, Si Meng, Tiantian Kong
Pages 350-360

View PDF Article preview

Review article *Open access*

Microalgae-based drug delivery systems in biomedical applications

Hui Huang, Yutong Lang, Shoujie Wang, Min Zhou
Pages 361-374

View PDF Article preview

Review article *Open access*

Cross-talk between biometal ions and immune cells for bone repair

Shubo Liu, Zhengjie Lin, Wei Qiao, Bin Chen, Jie Shen
Pages 375-408

View PDF Article preview

Full Length Article

Research article *Open access*

Ginsenoside Rb_1 improves human nonalcoholic fatty liver disease with liver organoids-on-a-chip

Hui Wang, Yue Zhu, Pengcheng Shi, Xiangyang Li, ... Guoping Zhao
Pages 283-294

View PDF Article preview

Research article *Open access*

Suppression of NFATc1 through NF-kB/PI3K signaling pathway by Oleandrin to inhibit osteoclastogenesis and bone resorption

Zhikun Li, Kai Chen, Qifeng Yu, Yifan Li, ... Wei Xu
Pages 342-349

View PDF Article preview

Research article *Open access*

Development of Muscle Tendon Junction in vitro Using Aligned Electrospun PCL Fibres

FEEDBACK

Nodoka Iwasaki, Marta Roldo, Aikaterina Karali, Alberto Sensini, Gordon Blunn
Pages 409-420

View PDF Article preview

Research article *Open access*

Immobilization of hUC-MSCs conditioned medium on 3D PLLA collagen-coated matrix enhances diabetic wound healing progression

Siufui Hendrawan, Olivia Marcelina, Sukmawati Tansil Tan, Hans Ulrich Baer
Pages 421-431

View PDF Article preview

Previous vol/issue Next vol/issue

ISSN: 2666-1381

Engineered Regeneration 5 (2024) 421–431

Contents lists available at ScienceDirect

Engineered Regeneration

journal homepage: http://www.keaipublishing.com/en/journals/engineered-regeneration/

Immobilization of hUC-MSCs conditioned medium on 3D PLLA collagen-coated matrix enhances diabetic wound healing progression

Siufui Hendrawan[a,b], Olivia Marcelina[a], Sukmawati Tansil Tan[c,*], Hans Ulrich Baer[d,e]

[a] Tarumanagara Human Cell Technology Laboratory, Faculty of Medicine, Tarumanagara University, Jakarta 11440, Indonesia
[b] Department of Biochemistry and Molecular Biology, Faculty of Medicine, Tarumanagara University, Jakarta 11440, Indonesia
[c] Department of Dermato-venereology, Faculty of Medicine, Tarumanagara University, Jakarta 11440, Indonesia
[d] Baermed, Centre of Abdominal Surgery, Hirslanden Clinic 8032 Zürich, Switzerland
[e] Department of Visceral and Transplantation Surgery, University of Bern, Switzerland

ARTICLE INFO

Keywords:
PLLA matrix
Diabetic wound
Conditioned medium
Human umbilical cord
Mesenchymal stem cell

ABSTRACT

Conditioned medium (CM) derived from human umbilical cord-mesenchymal stem cells (hUC-MSCs) which contains numerous amounts of growth factors, has demonstrated potential in treatment of diabetic wounds. However, for practical application, a biodegradable supporting material is needed to hold the CM and fill in the injury site, where deep cavity wounds are often present in diabetic patients. Poly-L-lactic acid matrix coated with collagen (PLLA/CC) is a suitable carrier due to its biodegradability and biocompatibility. Thus, we present a method to immobilize the hUC-MSCs CM on PLLA/CC through freeze-drying process (PLLA/CC CM FD). When seeded on PLLA/CC CM FD, fibroblasts had an increased cellular function in producing collagen; although no enhancement in cell viability was observed. Moreover, implantation of PLLA/CC CM FD on the wound of diabetic rats showed improvement in wound closure and collagen deposition in the wound area. Altogether, this study exhibits the potential of PLLA/CC CM FD as a therapy for diabetic deep cavity wound.

1. Introduction

Diabetes mellitus (DM) is associated with various complications, with one of the most frequent incidences is non-healing wounds. As per 2021, there are 537 million people suffering from diabetes, that is 10.5 % of the world population, and its prevalence is expected to rise in the upcoming years, along with the incidence of diabetic wounds [1]. Intriguingly, about 19 to 34 % people with diabetes are likely to suffer from foot ulcers as well [2]. On top of that, even with current therapies, diabetic wounds are still difficult to manage, leading to other complications and reduced quality of life for the sufferers.

The aberrative pathophysiology of non-healing wounds in DM is caused by hyperglycemia, which leads to alterations in terms of immune status, endothelial and neural functions [3]. Growth factors responsible for wound healing are found to be suppressed, both in pre-clinical and clinical findings. A study showed that hyperglycemic state destabilizes hypoxia inducible factor-1 (HIF-1), the key transcriptional activator of numerous growth factors. As the consequence, HIF-1-related downstream factors are failed to be amplified, these include vascular endothelial growth (VEGF), platelet-derived growth factor (PDGF), and fibroblast growth factor (FGF). This alteration is suggested to be the main factor underlying cellular irresponsiveness under diabetic injury [4,5]. Studies using diabetic animal models have shown that poor wound vascularization in diabetes is linked with down regulation of VEGF [5], keratinocyte growth factor (KGF) [6], basic fibroblast growth factor (bFGF) [7], hepatocyte growth factor (HGF) [8], and many other growth factors. Ultimately, these non-healing wounds might extend below the subdermal layers of the skin, creating cavity wounds, and expose the affected underlying tissues and structures, *e.g.*, bones, muscles, or tendons. Also, these wounds are mostly present with high amount of exudates, which substantially hampers a successful standard therapy [9,10].

Stem cell therapy has been long-known as a prospective approach to treat diabetic wounds. Several meta-analyses on completed clinical trials showed promising results of utilizing stem cells to treat diabetic wounds, especially diabetic foot ulcers [11–13]. Apart from their capabilities to differentiate and self-renew, stem cells possess another remarkable property through its paracrine activity. Stem cells are able to secrete a vast amount of growth factors, cytokines, chemokines, and other bioactive components into their cultured medium, further termed as a conditioned medium (CM). The use of CM as a cell-free product could overcome the limitation of stem cell therapy, as stem cell still faces ethical controversies and known to have a low survival rate when transplanted into unfavorable environment, in most cases, unhealthy recipients [14].

A previous study found that intradermal administration of CM derived from human umbilical cord-mesenchymal stem cells (hUC-MSCs)

* Corresponding author: Department of Dermato-venereology, Faculty of Medicine, Tarumanagara University, Jl. Letjen S. Parman No. 1 11440 Jakarta, Indonesia.
E-mail address: sukmawati@fk.untar.ac.id (S.T. Tan).

https://doi.org/10.1016/j.engreg.2024.04.005
Received 15 February 2024; Received in revised form 22 April 2024; Accepted 24 April 2024
Available online 8 May 2024

could improve wound healing progression in diabetic rats, resulting better re-epithelization and fibroblast function in secreting collagen compared to antibiotic administration [15]. Similar finding is also mentioned by Fong *et al.* by using CM derived from human Wharton's Jelly stem cells. Increased re-epithelization, vascularity, and hair follicle, as well as improved healing rate were seen in diabetic wound murine model [16]. However, for diabetic deep cavity wound, a biomaterial scaffold (matrix) might be required to provide mechanical support of filling in or bridging the wound cavity. This scaffold may also be required to retain and sustained release the growth factors into the wound site.

3-Dimensional biomaterial matrix is growing popularity in recent years, with many advantages to offer. Functions as a scaffold, a 3D biomaterial matrix should be able to provide mechanical support for cells that mimics the extracellular matrix (ECM) naturally, an important feature lacking in 2D cell-culture. Some of the most frequently used material include Poly-l-lactic acid (PLLA) and poly lactic-co-glycolic acid (PLGA), as they are FDA-approved biodegradable materials regularly used for suture fabrication. Previously, we developed a 3D biomaterial matrix using PLLA synthetic polymer, coated with collagen layer. Our engineered matrix displayed great biocompatibility for hepatocytes, shown through high cell attachment rate and function to secrete albumin [17]. Furthermore, implantation of this cellularized scaffolds (autologous hepatocyte matrix) into liver cirrhosis patients showed clinically relevant improvements for some patients [18,19]. Our other studies also showed that implantation of matrix seeded with islet cells could alleviate the blood glucose level in diabetic rats, proving the matrix capability to deliver cells into implantation site [20].

As diabetic deep cavity wounds lack of tissue integrity and innate cell regeneration, we discern that our 3D PLLA collagen-coated matrix (PLLA/CC) holds a great potential as an adjuvant therapy for deep cavity wounds in DM patients. Other than providing appropriate cellular environment, PLLA/CC could be employed to effectively deliver growth factor-rich hUC-MSCs CM into diabetic wound. Nevertheless, preclinical research is necessary to find the technique to immobilize hUC-MSCs CM on the PLLA/CC matrix, further elucidating its biocompatibility against fibroblast cells and ultimately, its effectivity to heal diabetic wound.

In this study, we found a method to immobilize growth factor-rich CM onto a PLLA/CC matrix scaffold through freeze-drying process (PLLA/CC CM FD). This treated matrix might be able to stimulate the function of seeded fibroblasts in producing collagen, the predominant structural component of ECM. Next, we aimed to assess the efficacy of PLLA/CC CM FD *in vivo* by implanting the matrix into diabetic rats using wound splinting model; in which, silicone splint is used to fix and cover the wound area, as well as to prevent skin contraction. Hence, this model ought to simulate the wound healing progression occurring in human [21]. Knowing the importance of fibroblast in producing ECM for tissue regeneration [22], we also generated a cellularized matrix by seeding allogeneic fibroblasts into PLLA/CC CM FD, expecting this fibroblast-containing matrix could further boost the wound healing process when implanted into the wound area. Although more study needs to be conducted for clinical implementation, our present study discovers a novel 3D CM-immobilized matrix as a potential treatment for deep cavity wounds in diabetic patients.

2. Material and methods

2.1. Preparation of hUC-MSCs CM

2.1.1. Isolation of human umbilical cord

Conditioned medium (CM) was produced from mesenchymal stem cells (MSCs) derived from human umbilical cord (hUC) in Tarumanagara Human Cell Technology Laboratory (THCT Lab) [15]. The study was approved by Universitas Tarumanagara Human Research Ethics Committee (UTHREC No. PPZ20192062). Briefly, fresh umbilical cord was obtained from caesarean delivery with parental consent. The tissue was washed with Phosphate Buffered Saline (PBS; Sigma Aldrich, St. Louis, MO) supplemented with 1 % antibiotic-antimycotic solution (Ab/Am; Sigma Aldrich) and cut into small pieces. Afterwards, the tissues were transferred into culture flasks containing complete medium, consists of Minimum Essential Medium Alpha (MEMα; Gibco, Life Technologies, Grand Island, NY), 20 % fetal bovine serum (FBS; Gibco), and 1 % Ab/Am. MSCs were expanded and cultured until confluent.

2.1.2. Identification of hUC-MSCs

Characterization of hUC-MSCs was performed at Biotechnology Laboratory, Primate Research Centre, Bogor Agricultural University. hUC-MSCs were expanded until passage 3 and subjected to reverse-transcriptase polymerase chain reaction (RT-PCR) analysis. Specific cell markers for mesenchymal stem cells were analyzed, *i.e.* CD73 and CD105, using GAPDH as the housekeeping gene [15,23]. The primer sequences of CD73 are as follow: forward: GACCTGGCTTTGTGACAGCAA; reverse: CTGACCCTGAGTAATCATGTCAGTCT. The sequences of CD105 primer are: forward: GACTGTCTTCACGCGCTTGA; reverse: GGAAGGCACCAAAGGTGATG. As for GAPDH, the primer sequences are: forward: CGGATTTGGTCGTATTGG; reverse: TCAAAGGTGGAGGAGTGG [24].

2.1.3. Preparation of hUC-MSCs CM

hUC-MSCs were cultured until reaching 80 % confluence at passage 5 – 6. After that, the complete medium was replaced with serum-free medium before culturing the cells under hypoxic condition (5 % O_2) for 3 days, using Forma^{TM} Steri-Cycle^{TM} i160 Dual CO_2 incubator (Thermo Scientific, Waltham, MA). This hypoxic condition is known to facilitate an increased secretion of growth factors by hUC-MSCs [15]. Afterwards, the culture medium was collected, separated from cell pellet, and sterile-filtered using 0.22 μm filter to obtain hUC-MSCs CM. Sterility tests were performed using Thioglycollate, CASO, and Sabouraud Broth (Millipore, Sigma Aldrich), to ensure the absence of microorganisms and fungi growth. Endotoxin and mycoplasma detections were performed using Toxin Sensor^{TM} (GenScript, Piscataway, NJ) and Venor® GeMq One Step (Minerva Biolabs, Berlin, Germany) respectively, according to manufacturer instruction.

2.1.4. Growth factors content measurement

Quantification of the growth factors content in hUC-MSCs CM was conducted through enzyme-linked immunosorbent assay (ELISA), specifically basic Fibroblast Growth Factor (Human bFGF ELISA Kit; Sigma Aldrich), Procollagen I (Human PCI ELISA Kit; Elabscience, Wuhan, China), Vascular Endothelial Growth Factor (Human VEGF ELISA Kit; Thermo Scientific), and Hepatocyte Growth Factor (Human HGF ELISA Kit; Elabscience). Procedure was performed according to manufacturer's manual.

2.2. Fabrication of collagen-coated PLLA matrix (PLLA/CC)

Three-dimensional collagen-coated Poly-l-Lactide Acid (PLLA) sponge was produced according to previous studies [17,25–27]. PLLA was purchased from Lactel®l-PL (B6002–2), Evonik (Piscataway, NJ). Shortly, PLLA matrix was prepared through salt-leaching method, using NaCl as the porogen. The resulting PLLA sponge had the thickness of 2 mm and porosity of >90 % with pore size ranged from 355 to 425 μm. The matrix was cut into round shape with diameter of 10 mm. Collagen coating was then performed by soaking the PLLA matrix in 0.5 % (w/v) type I bovine dermis collagen solution (AteloCell®, Koken, Tokyo, Japan) under reduced pressure using a vacuum freeze dryer FDU-2200 (EYELA, Tokyo, Japan), so that the collagen solution could fill the pores of the sponges. Each PLLA/collagen sponges were then put onto a 100 μm cell-strainer and then centrifuged at 2000 G for 10 min at 4 °C to remove excess collagen liquid, creating a thin-layer of collagen on PLLA matrix. Subsequently, the sponge was freeze-dried under vacuum condition (<5 Pa) for at least 24 h. Then, this collagen-coated PLLA sponge

(PLLA/CC) underwent plasma treatment (plasma cleaning and activation) using a custom-made plasma treatment system (Diener Electronic GmbH, Ebhausen, Germany). This PLLA/CC matrix was further used as our standard matrix. Finally, sterilization process was done by treating the matrix with 30 % H_2O_2 (Merck, Sigma Aldrich), at 30 °C, for at least 15 min.

2.3. Mechanical compression test

Compression test was evaluated by placing PLLA/CC cylindrical matrix with 10 mm of diameter (n = 3) between two steel rods of a mechanical test instrument with dynamic force processor (Unipulse F381A, Tokyo, Japan). A vertical force was applied at a controlled speed of 100 rpm at room temperature. The compressive strength was obtained from the compressive force divided by the cross-sectional area. Strain was calculated by dividing the percentage of displacement by the original distance of sample. Modulus of elasticity was determined by the ratio of compressive strength over the change of deformed sample area at the end of compression test [28,29].

2.4. Matrix degradation test

In order to assess the degradation rate of standard PLLA/CC matrix, *in vitro* degradation test was performed according to Yoshioka et al. [30]. Shortly, sterile standard matrices (n = 3) were placed in tubes and soaked in sterile PBS (pH 7.4) under shaking of 80 rpm at 37 °C using orbital shaker. The upper three-fourth of PBS was aspirated and replaced with new PBS every week; the collected PBS was subjected to pH measurement to observe the pH changes caused by the degraded matrix. The mass of the matrix was weighed every 6 weeks, with timepoint of 6-, 12-, 18-, 24-, and 30 weeks. Prior to weight measurement, matrices were washed with deionized water, air-dried under a fume hood for 24 h, and finally, vacuumed for 72 h using a vacuum drying oven DP200 (Yamato Scientific, Tokyo, Japan). The weight loss (%) of matrix at every endpoint was calculated using a simple equation:

$$\left(W_0 - W_t\right)/W_0 \times 100\%;$$

W_0 is the initial weight and W_t is the final weight at the designated timepoint.

2.5. CM immobilization of PLLA/CC matrix

CM immobilization was conducted through four methods based on literatures (Fig. 1): CM freeze-drying (CM FD) [31], CM absorption (CM Abs) [32], collagen-CM mixture freeze-drying (Col-CM FD), and gelatin-CM mixture air drying (Gel-CM AD) [33]. Later, to choose the best CM immobilization method, *in vitro* trial was performed.

2.5.1. Procedure of CM immobilization: CM freeze-drying (CM FD)

PLLA/CC was soaked in 1 % CM (v/v; in MEMα) for 30 min under reduced pressure, followed by freeze-drying process under vacuum condition (<5 Pa) for at least 24 h. CM concentration of 1 % was used based on prior pilot study, in which, 1 % of CM was sufficient to affect fibroblasts growth. Plasma treatment and sterilization were then carried as previously described.

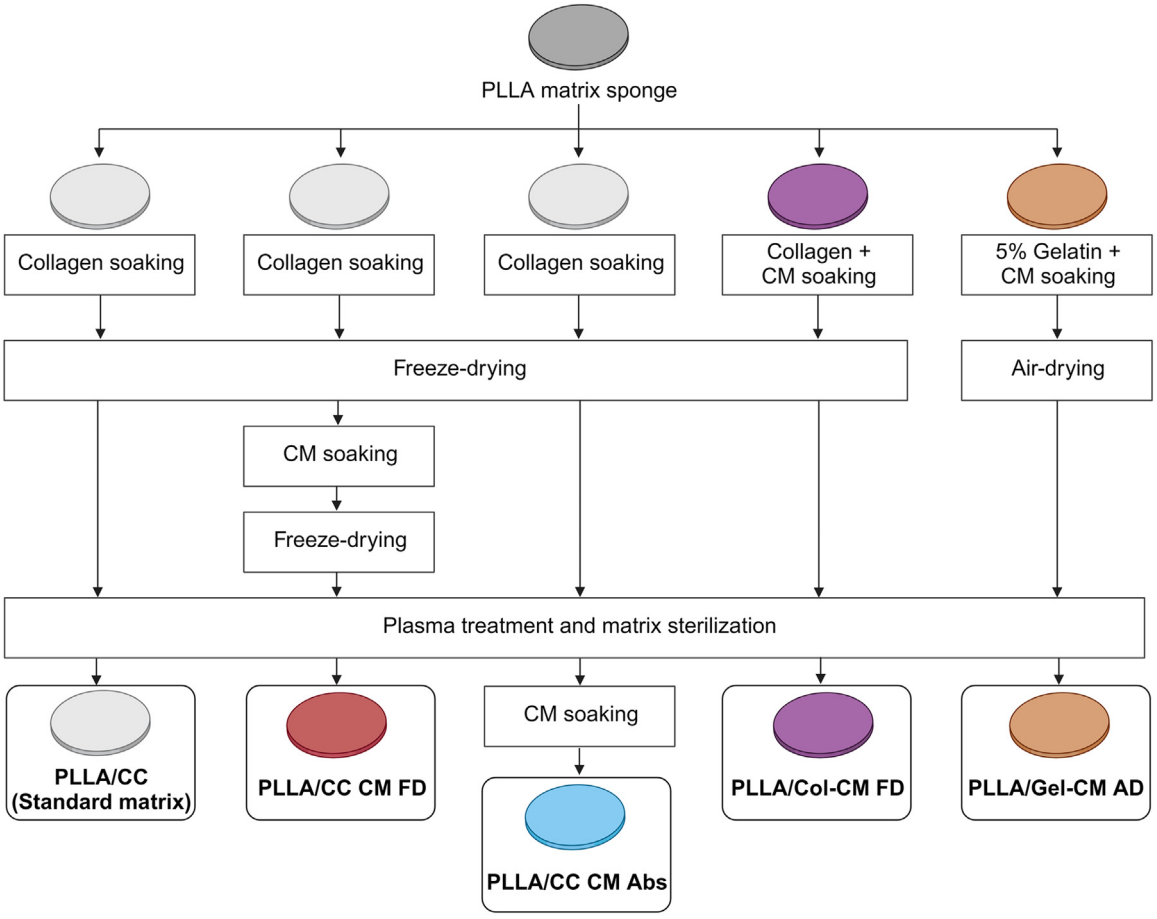

Fig. 1. Schematic diagram for techniques of CM immobilization on PLLA matrix. PLLA/CC: standard PLLA matrix coated with collagen solution; PLLA/CC CM FD: PLLA/CC immobilized with 1 % CM through freeze-drying; PLLA/CC CM Abs: PLLA/CC immobilized with CM through absorption; PLLA/Col-CM FD: PLLA immobilized with mixture of collagen and 1 % CM; PLLA/Gel-CM AD: PLLA immobilized with mixture of gelatin and 1 % CM.

2.5.2. Procedure of CM immobilization: CM absorption (CM abs)

Absorption of the PLLA/CC matrix in CM was done by soaking the sterilized PLLA/CC sponge in CM concentrate, shaken at 100 rpm, 37 °C for 24 h. Following the absorption process, the PLLA/CC CM Abs matrix was transferred into a new well-plate, prior to cell seeding.

2.5.3. Procedure of CM immobilization: collagen-CM freeze-drying (Col-CM FD)

Modified PLLA/CC coating procedure was carried; instead of coating with collagen only, the PLLA matrix sponge was soaked in a mixture of collagen and 1 % CM under reduced pressure. Afterwards, the freeze-drying procedure, plasma surface treatment and sterilization were performed as usual.

2.5.4. Procedure of CM immobilization: gelatin-CM air-drying (Gel-CM AD)

After salt-leaching procedure, the standard PLLA matrix was soaked in a mixture of 5 % gelatin (Sigma Aldrich) and 1 % CM under reduced pressure. The soaked matrix was then air-dried under a fume hood for 24 h and proceeded to plasma treatment and sterilization.

2.6. Isolation of fibroblasts

Primary rat dermal fibroblasts were isolated from male Sprague Dawley aged 12 weeks (National Agency of Drug and Food Control, Jakarta, Indonesia) according to previous study [17]. The isolation procedure was approved by the Institutional Animal Care and Use Committee (IACUC) of Tarumanagara University (IACUC No. 003.KEPH/UPPM/FK/VI/2019). Under deep anesthesia, full thickness abdominal skin (3 × 3 cm) was collected and subsequently washed with PBS containing 2 % Ab/Am for five times. Additional washing was performed using 0.5 mM ethylene glycol bis (2-aminoethyl ether)-N,N,N',N'-tetra acetic acid (EGTA; Sigma Aldrich) containing 2 % Ab/Am for another five times. Tissue was digested using 200 U/mL collagenase type I (Gibco) and incubated for 5 h at 37 °C, 5 % CO_2. Cells were gently scraped from the dermis side of the abdominal skin; cells were collected, sieved, and suspended in standard medium, that is Dulbecco's Modified Eagle's Medium (DMEM; Sigma Aldrich) containing 20 % FBS, 1 % sodium pyruvate (Sigma), 1 % 4-(2-Hydroxyethyl) piperazine-1-ethanesulfonic acid (HEPES; Sigma), and 1 % Ab/Am. Fibroblasts were cultured until 90 % of confluence and used afterwards for further *in vitro* and *in vivo* study as an allotransplant.

2.7. Cell culture and seeding

Fibroblasts were grown and cultured using standard DMEM medium. For experiments involving 3D matrices, cells were seeded on matrix (5×10^5 cells/matrix) by adding 100 μL of cell suspension into each matrix. As for control, which regarded as control 2D, cells were seeded directly into 12 well-plate with equal number of cells as in 3D matrix. For scratch wound assay, cells with 80 to 90 % confluency (2×10^5 cells/well) were seeded on a 6-well plate.

2.8. Cell viability assay

To detect viable cells adhering onto the matrix, cell viability assay was performed using Cell Counting Kit-8 (CCK-8; Sigma Aldrich) according to manufacturer's instruction. This assay was conducted to analyze the cyto-compatibility of the matrix to support fibroblast growth. Briefly, 24 h after the seeding, the culture medium was collected for further total collagen detection assay. Meanwhile, the matrix was transferred into a new well-plate prior to the addition of working medium to prevent the detection of cells attached on bottom of the well-plate (leaked cells). Working medium containing standard medium and CCK-8 solution (10:1) was added to each well and incubated in CO_2 incubator for 4 h at 37 °C. Afterwards, the absorbance was measured at 450 nm using a microplate reader (Multiskan EX, Thermo Scientific). Fibroblasts seeded in 2D well-plate format was used as the control. Results were expressed as relative number of viable cells compared to the control, which was assumed as 1.

2.9. Scratch wound assay

To evaluate the effect of CM on fibroblasts migration, a scratch wound assay was performed [34]. Shortly, 24-hours after seeding, the cells were cultured in starvation medium (DMEM without FBS) for 16–18 h to halt cell proliferation. Then, a scratch was applied on a monolayer confluent fibroblast and cells were washed with PBS to remove cell debris. For 1 %CM group, 1 % amount of CM was added into the medium. After 24 h, cells were fixed using 4 % paraformaldehyde and captured for further wound closure measurement using ImageJ software (National Institute of Health, Bethesda, MD):

$$\text{Wound closure}(\%) = \left(A_0 - A_t\right)/A_0 \times 100\%;$$

where A_0 is the initial wound area at D0 and A_t is the final wound area at endpoint.

2.10. Sirius red total collagen detection assay

In order to quantify the total collagen amount secreted by fibroblasts, culture medium was collected from each well after 24 h of fibroblast seeding. ELISA was performed using Sirius Red Total Collagen Assay Kit (Chondrex, Woodinville, WA) according to manufacturer's guidelines. Prior to ELISA assay, culture medium was centrifuged at 1000 G for 20 min to remove cell debris, followed by concentrating the sample using Concentration Solution (Chondrex) accordingly. The optical density (OD) was read at 530 nm.

2.11. Scanning electron microscope imaging

SEM analysis was carried to visualize the morphology of fibroblasts attached onto the PLLA/CC sponges. The protocol was done according to previous study [17]. Pre-treatment of the sample included sample washing in PBS and fixation in 3 % glutaraldehyde (Sigma Aldrich) for 2 h at 4 °C. Samples were then dehydrated using increasing concentration of ethanol up to 100 % at room temperature. Afterwards, samples were chemically dried with hexa-methyl disilizane (HMDS; Sigma Aldrich) for 24 h at room temperature. Samples were coated using Fine Coater JFC 1600 (JEOL, Tokyo, Japan) and visualized with JEOL JSM 6510-LA Scanning Electron Microscope (JEOL). Energy Dispersive Spectroscopy (EDS) detection was conducted to determine elemental content of the sample. Latter protocol was performed in SEM Laboratory, Faculty of Mathematics and Natural Sciences, Bandung Institute of Technology, Bandung, Indonesia.

2.12. Animal experiment

Male Sprague Dawley rats aged 14-week-old (150–180 g) were obtained from National Agency of Drug and Food Control, Jakarta, Indonesia. All procedures were conducted in PT Bimana Indomedical, Bogor, West Java, Indonesia following the protocols accepted by the Animal Care and Use Review Committee of Bimana Indomedical Corporation (ethical approval number R.05–22-IR). The number of animals was determined using ANOVA Resource Equation formula, considering the 3Rs principle (Replacement, Reduction, and Refinement) [35]. Rats were housed under controlled temperature, humidity, and lighting (12-hour light/dark cycle) with *ad libitum* feeding; rats were acclimatized for one-week post-arrival.

2.12.1. Induction of diabetic rats

Diabetes model was established through a streptozotocin (STZ) injection according to our previous study [15]. STZ (Sigma Aldrich S0130)

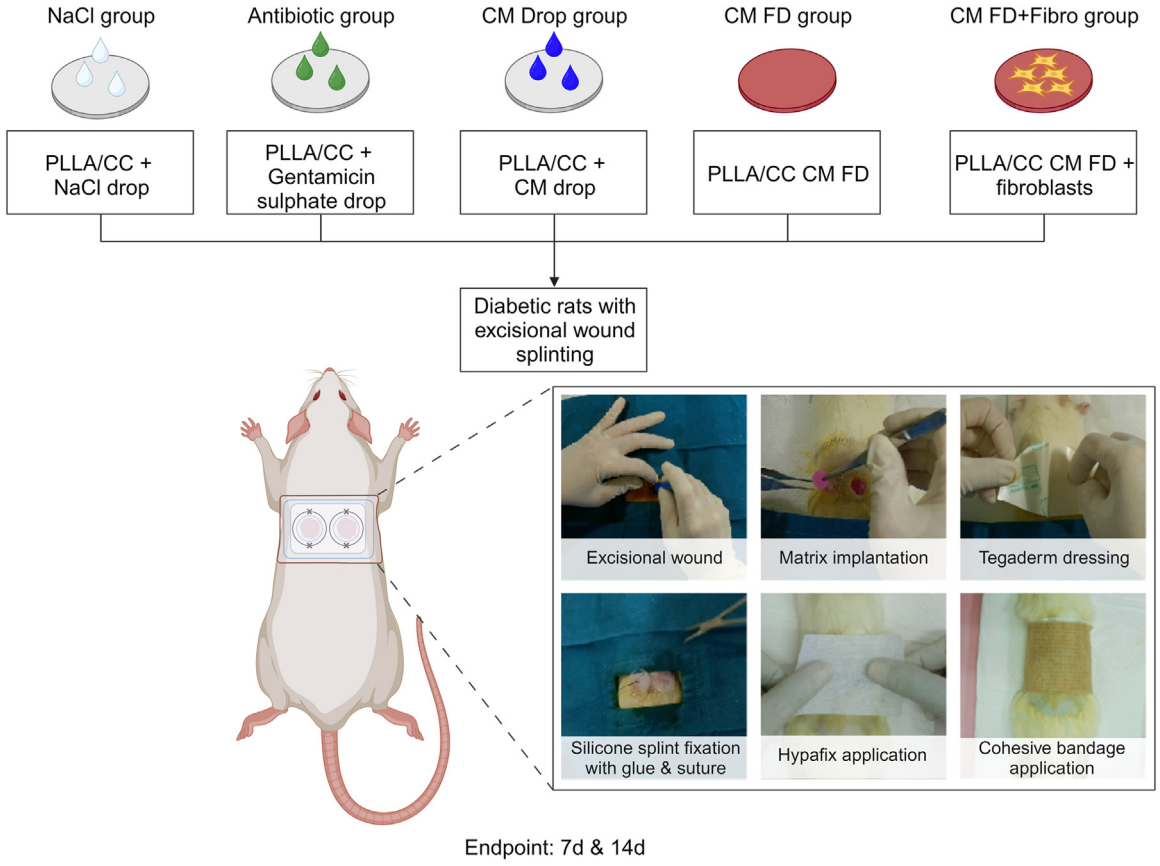

Fig. 2. Schematic diagram for matrix implantation grouping onto diabetic rats with excisional wound splinting model.

was freshly prepared in citrate buffer pH 4.0 prior to single intraperitoneal injection of 50 mg/kg BW [36]. As the baseline, fasting blood glucose level was measured through tail prick method using GlucoDr. (All Medicus, Anyang, South Korea) before diabetes induction. At 9th day post induction, fasting blood glucose level was measured again; rats were confirmed as diabetic with the blood glucose level of >200 mg/dL.

2.12.2. Establishment of excisional wound splinting model

Excisional wound splinting model was created on diabetic-induced rats according to protocols conducted by Wang *et al.* [21] and Shin *et al.* [37]. Briefly, rats were anesthetized through intraperitoneal injection of ketamine 10 % (40–80 mg/kg; Kepro, Woerden, Netherlands) and xylazine 2 % (5–10 mg/kg; Xyla, Interchemie, Hapert, Netherlands) as previously described [15]. Two full thickness skin wounds (diameter 8 mm each) were created on dorsal side of each rat using a biopsy puncher (Fig. 2). Rats (n = 2) were grouped randomly to receive implantation of matrices on the wound site. As the control group, standard PLLA/CC matrix added with 0.2 mL NaCl dropwise was implanted into the wound site. Antibiotic group was treated with PLLA/CC matrix added with 0.2 mL Gentamicin Sulphate dropwise (40 mg/mL; Sagestam®, Sanbe, Bandung, Indonesia). As for CM-treated groups, divided into: 1) CM Drop group were implanted with standard PLLA/CC matrix added with 0.2 mL CM drop by drop; 2) CM FD group was treated with PLLA/CC CM FD matrix; and 3) CM FD+Fibro group was implanted with PLLA/CC CM FD seeded with fibroblasts obtained from a donor rat (5×10^5 cells/matrix). Subsequently, all wounds were closed with Tegaderm transparent dressing (3 M, St. Paul, MN). Silicone splints (diameter 19 mm) were fixed upon the wound area (wound splinting) using adhesive glue and 6–0 nylon suture (Ethilon®, Ethicon, Raritan, NJ) at 2 points. Afterwards, a non-woven dressing (Hypafix®, Essity, Stockholm, Sweden) was applied across both wounds and enclosed with a cohesive bandage.

2.13. Wound closure measurement

Wound area was captured and measured at two endpoints: 7- and 14-days post wound splinting procedure. The area of the wound was determined by tracing the outer margin of the wound using ImageJ software [38]. The percentage wound closure was calculated using the wound closure equation at indicated endpoints, as previously described.

2.14. Histopathological analysis

At endpoint (14 days post wound splinting procedure), rats were euthanized and full-thickness skin specimens were collected. Specimens were fixed in 4 % paraformaldehyde and afterwards, histochemical staining was performed by the Pathology and Anatomy Laboratory, Primate Research Centre, Bogor Agricultural University. Tissue specimens were subjected to Hematoxylin & Eosin (H&E) staining to determine the width of re-epithelization, which results were represented as the ratio of re-epithelization length over total length of the wound. Masson's Trichome staining (MT) was also performed to obtain the area of collagen deposit, which data were expressed as the ratio of collagen deposit area over total skin tissue area. Section images were obtained with Nikon Eclipse 80i microscope (Nikon, Tokyo, Japan). Quantification was done using ImageJ software.

2.15. Statistical analysis

All results were expressed as means ± SD. Wound closure percentage between two time points was analyzed using mixed- Analysis of Variance (ANOVA). Quantification of histopathological analysis was evaluated using Kruskal-Wallis. Other experiments were evaluated using one-way ANOVA. $^{*}p < 0.05$ was considered as significantly different, while $^{**}p < 0.01$ was defined as highly significance.

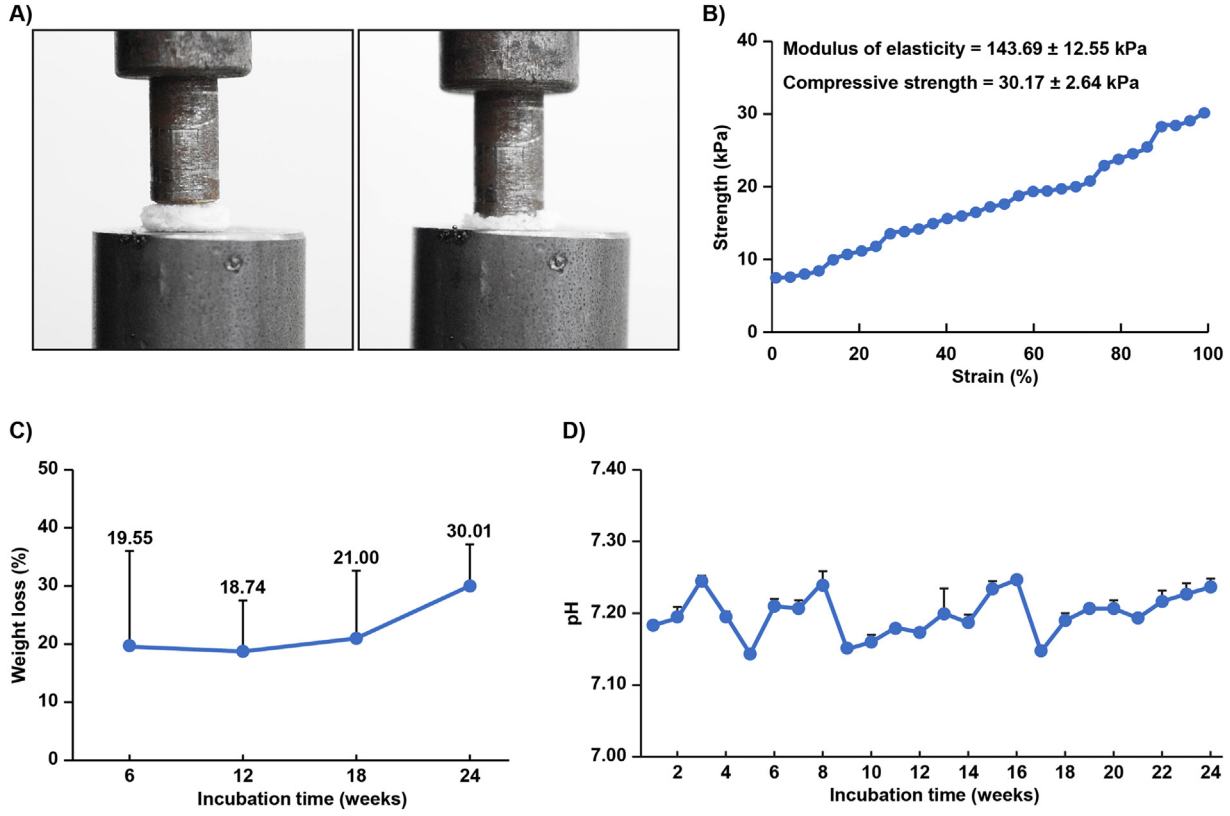

Fig. 3. Mechanical and degradation properties of PLLA/CC matrix. (A) Compression testing process of PLLA/CC. (B) Strength-strain curve of PLLA/CC. (C) The weight loss of PLLA/CC matrix in PBS over 24 weeks. (D) Changes in environmental pH of PLLA/CC matrix over 24 weeks . Data were presented as means ± SD ($n = 3$).

3. Results

3.1. Mechanical and biological properties of PLLA/CC

As the standard matrix, PLLA matrix was prepared using salt-leaching method, subsequently coated with collagen through freeze-drying process, further designated as PLLA/CC matrix. PLLA/CC intended to act as cellular support, which mimics natural extracellular matrix [17,39]. Compression test showed that PLLA/CC had a compressive strength of 30 kPa with elastic modulus of 143 kPa (Fig. 3A-3B). The relatively low mechanical strength of matrix is due to the highly porous state of PLLA/CC, that is >90 %. In comparison, another study also stated the low mechanical strength of PLLA scaffold with 80 % porous content, that was 0 ~ 5000 kPa. At the same time, low elasticity of PLLA/CC might be due to the brittleness of PLLA material [40], although PLLA/CC was more elastic than that of porous scaffold made of collagen only, with Young's modulus of 23.6 kPa [29].

While PLLA/CC had low mechanical strength, this feature might take part in its ability to degrade. Degradation test showed that PLLA/CC matrix had an increasing weight loss over incubation time, reaching about 30 % of loss at week 24 (Fig. 3C). During these 24 weeks, the pH value remained particularly stable, that was in the range of 7.17–7.24 (Fig. 3D). Although lower than the original pH of PBS (7.4), the pH decrease resulted by PLLA/CC matrix was still in compliance with the range of physiological pH for most tissues in human (7.0 – 7.4) [41].

Moreover, PLLA/CC poses great biocompatibility against fibroblasts. After 24 h of seeding, the fibroblasts were able to attach and spread inside the pores of PLLA/CC; present with round and spindle-shaped, elongated morphologies (Fig. 4A-4B). This conforms with our previous finding, indicating that PLLA/CC had 70 % of adherence rate against rat dermal fibroblasts [17]. Energy dispersive spectroscopy (EDS) analysis further showed the element constituent of PLLA/CC, which is dominated by carbon (C), followed by oxygen (O) (Fig. 4C). Therefore results above depicted the properties of PLLA/CC, although had low mechanical property, PLLA/CC had a proven degradability and biocompatibility against fibroblasts.

3.2. Immobilization of CM on PLLA/CC matrix promotes collagen secretion of fibroblasts

Previously, we found that conditioned medium derived from human umbilical cord mesenchymal stem cells (hUC-MSCs CM) could enhance the wound healing progression in diabetic rats [15]. Subsequent to hUC-MSCs isolation, RT-PCR screening confirmed the isolated hUC-MSCs to be positive of CD73 and CD105, main surface markers for hUC-MSCs (Supplementary Fig. S1). Furthermore, CM collected from hUC-MSCs contained a robust amount of growth factors, particularly basic fibroblast growth factor (bFGF), procollagen I (PCI), vascular endothelial growth factor (VEGF), and hepatocyte growth factor (HGF) (Supplementary Fig. S2A). This CM could also promote the migration potential of fibroblasts (Supplementary Fig. S2B, S2C), which is one important factor to accommodate the formation of ECM in the wound site [22]. However, despite of aforementioned favorable properties of hUC-MSCs CM, to maintain the CM in deep cavity wounds, a scaffold is required to provide the mechanical support and sustained CM delivery. Therefore, we aim to immobilize the hUC-MSCs CM on our 3D biodegradable and biocompatible PLLA/CC matrix.

Among four different CM immobilization techniques, *in vitro* biocompatibility test for each matrix was performed through CCK-8 assay. After 24 h, CCK-8 results showed that PLLA/CC CM FD had the most prominent viable cells among other immobilization techniques. However, it is noteworthy that fibroblasts seeded in all 3D matrices had lower viability than cells grown in 2D format (well-plate) (Fig. 5A). At the same time, cells grown in PLLA/CC CM FD and PLLA/Col-CM FD showed improve-

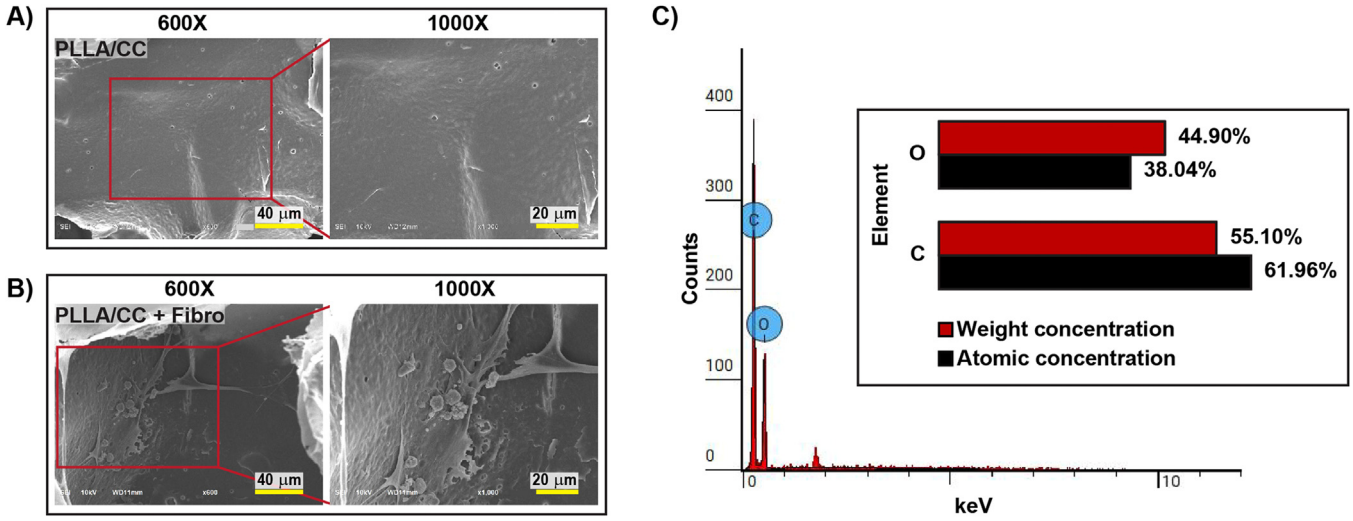

Fig. 4. Biocompatibility and chemical property of PLLA/CC matrix for fibroblasts growth. (A) Representative SEM images of cell-free PLLA/CC matrix and (B) fibroblasts-loaded PLLA/CC matrix. Left panels show 600x magnification (scale bar: 40 µm) with red boxes indicate the focus area for 1000x magnification; right panels show 1000x magnification (scale bar: 20 µm). (C) Energy Dispersive Spectroscopy detection of PLLA/CC; element code "C" stands for Carbon, "O" stands for oxygen.

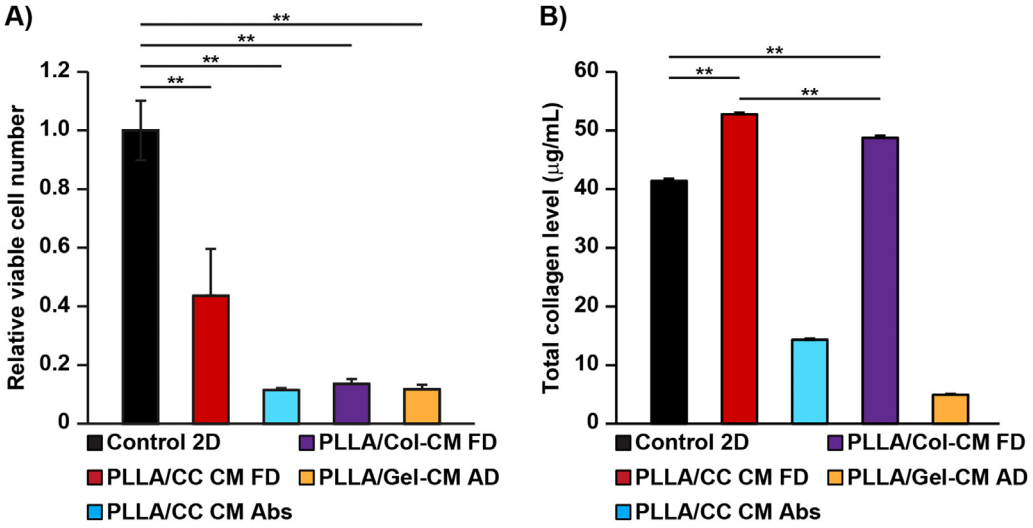

Fig. 5. Viability and collagen secretion of fibroblasts on PLLA matrices immobilized with hUC-MSCs CM. (A) Viability of fibroblasts seeded on PLLA matrix with different CM immobilization methods, as examined using CCK-8 assay ($n = 3$). (B) Total collagen production of fibroblasts on different PLLA matrices immobilized with CM, as determined by ELISA ($n = 5$). All experiments were done at 24 h after seeding. Data were shown as means ± SD (**$p < 0.01$). Control 2D: cells seeded on well-plate; PLLA/CC CM FD: PLLA matrix coated with collagen solution and immobilized with CM through freeze-drying; PLLA/CC CM Abs: PLLA matrix coated with collagen solution and immobilized with CM through absorption; PLLA/Col-CM FD: PLLA matrix immobilized with mixture of collagen and CM; PLLA/Gel-CM AD: PLLA matrix immobilized with mixture of gelatin and CM.

ment in their capacity to produce total collagen protein, compared to control 2D (Fig. 5B). Although a thin-layered collagen in the PLLA/CC matrix might also contribute to the collagen quantification, this result depicted that fibroblast grown in PLLA/CC CM FD showed the most prominent level of total collagen production compared to other groups, and therefore selected for further study.

3.3. PLLA/CC CM FD accelerates wound healing progression in diabetic rats

In order to assess the efficacy of PLLA/CC CM FD for diabetic wound healing, *in vivo* study was carried using excisional wound splinting model on diabetic Sprague Dawley rats. All rats were confirmed as diabetic (fasting blood glucose level >200 mg/dL) and showed a significant body weight decrement after streptozotocin injection (Supplementary Table S1), which conformed to pathophysiological states of diabetes [36].

Visually, wounds in diabetic rats were present with exudates and poor complexions (Fig. 6A). After 7 days of implantation, the CM Drop group showed the highest tendency of wound closure percentage (10.85 % ± 17.76 %), although not statistically significant among other groups (Fig. 6B). However, after 14 days, CM FD group showed the highest wound closure percentage, reaching more than 30 % of mean wound closure percentage. The mean wound closure percentage of CM FD group was significantly higher compared to NaCl group ($p = 0.018$) and CM FD+Fibro groups ($p = 0.046$). Intriguingly, in contrast to our hypothesis, CM FD+Fibro groups showed no improvement in wound closure percentage.

Subsequently after 14 days of implantation, H&E staining was performed to determine the fibroblast count and observe skin re-

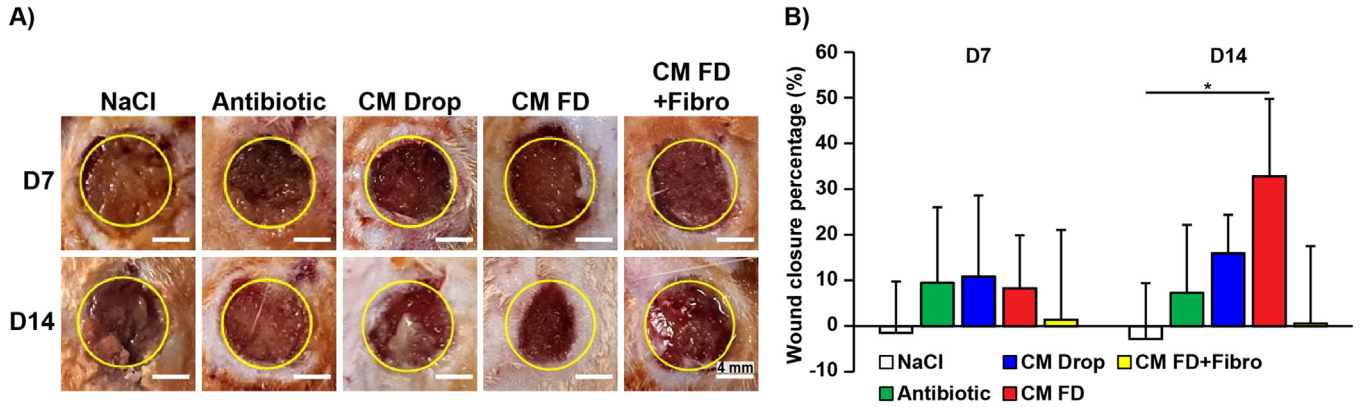

Fig. 6. Wound closure of diabetic rats following matrix implantation. (A) Representative images of wound closure in diabetic rats at 7- and 14 days following wound splinting establishment and treatment (scale bar: 4 mm); yellow circle indicates the initial wound size with diameter of 8 mm. (B) Quantification of wound closure percentage compared to initial wound area ($n = 4$). Data were shown as means ± SD (*$p < 0.05$). NaCl: PLLA/CC implant with NaCl drops; Antibiotic: PLLA/CC matrix implant with gentamicin sulphate drops; CM Drop: PLLA/CC implant with CM drops; CM FD: PLLA/CC CM FD implant; CM FD+Fibro: PLLA/CC CM FD implant seeded with fibroblasts.

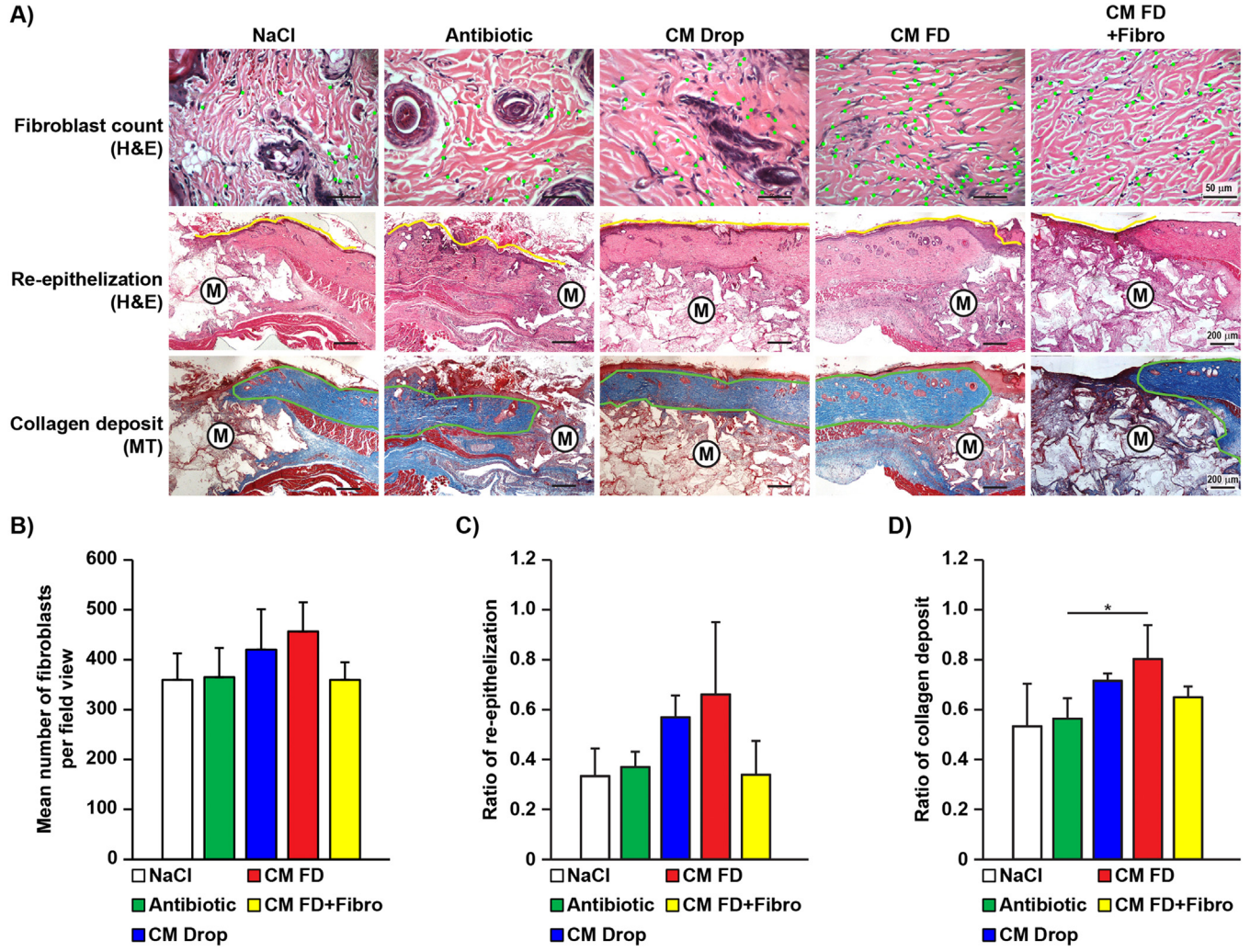

Fig. 7. Wound healing progression of diabetic rats following matrix implantation. (A) Representative images of histopathology analysis for fibroblast count (H&E staining, indicated by green dots; upper panel, scale bar: 50 μm), re-epithelization (H&E staining, indicated by yellow line; middle panel, scale bar: 200 μm), and collagen deposit area (MT staining, green line; lower panel, scale bar: 200 μm) in wound area of diabetic rats 14 days following wound splinting establishment and treatment. Implanted matrix is indicated by "M". (B) Mean number of fibroblasts count in 10 field views ($n = 4$). (C) *Re*-epithelization length ratio over total wound length ($n = 4$). (D) Collagen deposit ratio over total skin tissue area ($n = 4$). Data were expressed as means ± SD (*$p < 0.05$ *vs*. Antibiotic). NaCl: PLLA/CC implant with NaCl drops; Antibiotic: PLLA/CC matrix implant with gentamicin sulphate drops; CM Drop: PLLA/CC implant with CM drops; CM FD: PLLA/CC CM FD implant; CM FD+Fibro: PLLA/CC CM FD implant seeded with fibroblasts.

epithelization, while MT staining was done to analyze the total collagen deposit for wound tissue. In line with above results, histopathological analysis showed similar tendencies (Fig. 7). CM FD group had the highest score of fibroblast count and re-epithelization, as well as significantly higher area of collagen deposit, compared to Antibiotic group ($p = 0.034$).

4. Discussion

Current standard care for diabetic wound is still considered insufficient and often ends with poor prognosis, due to abnormal wound healing process in diabetes. Adjuvant therapy is required to complement the standard care, to support endogenous healing capabilities in diabetic patients [42]. Previously, we found that conditioned media obtained from human umbilical cord mesenchymal stem cells (hUC-MSCs CM) could improve wound progression in diabetic rats [15], which might attribute to the high concentration of several GFs, including VEGF, HGF, bFGF, and PCI. VEGF is renowned as the key promoter of angiogenesis process required to initiate vessel formation [43]. VEGF works synergistically with HGF in enhancing endothelial function, as HGF is the mitogen for endothelial cells [44]. It promotes fibroblast proliferation and migration, inducing collagen deposition and epithelization [43], which is in accordance with our finding that hUC-MSCs CM also stimulates the migration potential of fibroblasts. At the same time, bFGF is known as a potent stimulator for angiogenesis, by promoting endothelial cells mitogenesis and fibrocytes function [45]. Meanwhile, procollagen I is the precursor of collagen type I and its presence is correlated with collagen synthesis, found during tissue granulation in wound healing process [46].

Although hUC-MSCs CM could be effective for wound healing stimulation, a scaffold is required to deliver and retain the CM in the wound area, as diabetic wounds are often present in the form of deep cavities [31,32]. Herein, we develop a collagen-coated PLLA 3D matrix (PLLA/CC) to provide structural and functional support for wound cavity closure process. Our PLLA/CC presents with weak mechanical strength and elasticity, and hence, easily deformed. Nevertheless, PLLA/CC low mechanical property might contribute to its ability to degrade, with 18 % of weight loss after 12 weeks and 30 % loss after 24 weeks. Meanwhile, others reported the PLLA degradation of 23 % after 12 weeks [47] and 15 % after 26 weeks [30]. Faster degradation rate might be due to the matrix porous structure, collagen coating, and plasma treatment to PLLA/CC, which converts the hydrophobic PLLA into a more hydrophilic material and speed up surface erosion of the entire matrix [17,47,48]. It is notable that *in vivo* degradation rate could be faster due to the plasma content and enzymatic process to accelerate the degradation [49].

During the degradation of PLLA/CC, the environmental pH is mainly stable while still in the range of physiological pH (7.17 – 7.24). In contrast, PLLA-based scaffold is known to undergo hydrolytic degradation into lactic acid, and these acid by-products hardly diffuse out of the matrix and are accumulated within the PLLA interior in bulk. As the matrix degrades, the acidic monomers are then burst released to the system environment, leading to environmental pH drop, which could induce inflammatory response in recipient body system [47,48]. In this regard, weekly replacement of 75 % PBS volume might prevent the pH drop. Still, if significant pH drop ought to happen, the resultant pH will further decrease regardless of PBS replacement. Furthermore, in terms of biocompatibility, PLLA/CC shows great biocompatibility against fibroblasts. Overall, although PLLA/CC possesses weak strength and elasticity, the main purpose of the matrix is to act as a provisional matrix for cells to reside, proliferate and migrate, facilitating wound healing process while retaining the hUC-MSCs CM.

Next, we immobilize hUC-MSCs CM into PLLA/CC matrix through freeze-drying process, modifying the method from Horimizu *et al.* [31] (further mentioned as PLLA/CC CM FD). Interestingly, fibroblast grown in 3D PLLA/CC CM FD has a significant lower cell number, while exhibiting a more robust collagen production compared to 2D well-plate culture. Similar with our finding, MSCs grown in 3D gelatin/poly caprolactone electro spun fiber also had a lower viability compared to 2D culture. However, secretory function of MSCs in 3D culture increased significantly, in particular, factors playing important roles in tissue regeneration, *i.e.*, bFGF and HGF [50]. This phenomenon might be due to the homogenous distribution of nutrition and oxygen in 2D culture system. Still, 2D culture hardly represents the actual *in vivo* cellular environment, as well as cellular bioactivity [51]. Taken together, the PLLA/CC CM FD displays the capacity to carry and importantly, enhance fibroblast function, at least in producing collagen.

To further determine the efficacy of PLLA/CC CM FD, we performed *in vivo* study using excisional wound splinting model in diabetic rats. PLLA/CC CM FD matrix was implanted with or without fibroblast cells and as the comparison, we also implanted PLLA/CC matrices dripped with NaCl, antibiotic, or CM to other groups. All groups show no significant improvement of wound closure at 7 days-post implantations. At 14th day, implantation of PLLA/CC CM FD indicates the most profound wound closure percentage in diabetic rats, that is about 32 %. Concomitantly, PLLA/CC CM FD also demonstrates the highest collagen deposit area at 14 days, in line with the *in vitro* study. Higher re-epithelization and fibroblast count are also observed in wound tissue of PLLA/CC CM FD.

In contrast to our hypothesis, implantation of cellularized PLLA/CC CM FD (seeded with fibroblasts) does not improve the outcome. PLLA/CC CM FD+Fibro involves the loading of cell suspension into the matrix and further culturing process for 24 h, producing an implant with more liquid content compared to other matrix implants. It is plausible that PLLA/CC CM FD+Fibro implant interferes the healing process, as diabetic wound generally produces excess exudates [52]. Therefore, effective diabetic wound reinforcement also requires a type of therapy/dressing which could absorb the excessive fluid [53]. It is also noteworthy that PLLA/CC CM FD+Fibro contains allogeneic fibroblasts, which might raise immune rejection and impede wound healing process [54,55]. In this respect, the use of PLLA/CC CM FD+Fibro, might not be an ideal therapy for diabetic wound. Meanwhile, non-cellularized PLLA/CC CM FD is present as a dry porous matrix and more likely to play a better role to support cell function in diabetic wound area. High content of GFs in CM hUC-MSCs, immobilized all over the PLLA/CC matrix, might account for the wound healing process by PLLA/CC CM FD implant.

Treatments for hard-to-heal wound are broadly available, consisting of debridement, dressing, decompression, or application of GFs [56]. Utilization of stem cells and its derivates, such as conditioned medium or exosomes, has been extensively studied in search for optimum diabetic wound treatment. However, in spite of their potent activity, effective mode of delivery is prerequisite to ensure a maximum retention. Ultimately, the main goal is to promote patient tissue regeneration in wound healing process [57,58]. PLLA/CC CM FD is a potential 3D matrix carrying robust angiogenic GFs, with biodegradable and biocompatible profiles. Although more research is required, PLLA/CC CM FD offers a new insight for novel treatment of diabetic wound, especially ones with deep cavities.

5. Conclusion

Deep cavity wound in diabetic patients poses a great challenge to healthcare systems, where current standard care is mostly insufficient to induce a proper healing. Through our study, we present a potential therapeutic agent, PLLA/CC CM FD, a 3D PLLA matrix immobilized with hUC-MSCs CM, in which the CM itself contains a robust amount of growth factors. This porous matrix is biodegradable and could act as the structural support for cells to grow. Moreover, *in vivo* study confirms the effectivity of PLLA/CC CM FD to promote wound healing in diabetic rats, which suggests more research to be done for further potential application in diabetic wound.

Ethics approval and consent to participate

Human umbilical cord was collected and processed in accordance with the institutional approval from Universitas Tarumanagara Human Research Ethics Committee (UTHREC No. PPZ20192062). All animal procedures and protocol were approved by the Institutional Animal Care and Use Committee (IACUC) of Tarumanagara University (IACUC No. 003.KEPH/UPPM/FK/VI/2019) and ACUC of Bimana Indomedical Corporation (ethical approval number R.05–22-IR).

Declaration of competing interest

HUB has an interest in intellectual properties in tissue engineering. Other authors they declare that they have no known competing financial interests or personal relationships that could have appeared to influence the work reported in this paper.

Acknowledgments

This study was funded by grants from the Ministry of Research Technology and Higher Education, Jakarta, Indonesia (3499/LL3/KR/2021 and 470/LL3/AK.04/2022); and supported by Baermed, Center of Abdominal Surgery, Zurich, Switzerland. The authors also acknowledge Bimana Indomedical Corporation (Bogor, Indonesia); and Assoc. Prof. Erwin Siahaan (Faculty of Mechanical Engineering, Tarumanagara University, Indonesia) for kindly providing the mechanical compression testing.

Supplementary materials

Supplementary material associated with this article can be found, in the online version, at doi:10.1016/j.engreg.2024.04.005.

References

[1] IDF, IDF Diabetes Atlas: 10th Edition, 10th ed., Brussels, 2021.
[2] D.G. Armstrong, A.J.M. Boulton, S.A. Bus, Diabetic foot ulcers and their recurrence, N. Engl. J. Med. 376 (2017) 2367–2375, doi:10.1056/nejmra1615439.
[3] M. Mieczkowski, B. Mrozikiewicz-Rakowska, M. Kowara, M. Kleibert, L. Czupryniak, The problem of wound healing in diabetes—From molecular pathways to the design of an animal model, Int. J. Mol. Sci. 23 (2022) 7930, doi:10.3390/ijms23147930.
[4] K.Y. Howangyin, J.S. Silvestre, Diabetes mellitus and ischemic diseases, Arterioscler. Thromb. Vasc. Biol. 34 (2014) 1126–1135, doi:10.1161/ATVBAHA.114.303090.
[5] H. Thangarajah, D. Yao, E.I. Chang, Y. Shi, L. Jazayeri, I.N. Vial, R.D. Galiano, X. Du, R. Grogan, M.G. Galvez, M. Januszyk, M. Brownlee, G.C. Gurtner, The molecular basis for impaired hypoxia-induced VEGF expression in diabetic tissues, Proc. Natl. Acad. Sci. 106 (2009) 13505–13510, doi:10.1073/pnas.0906670106.
[6] C. Peng, B. Chen, H.K. Kao, G. Murphy, D.P. Orgill, L. Guo, Lack of FGF-7 further delays cutaneous wound healing in diabetic mice, Plast. Reconstr. Surg. 128 (2011) 673e–684e, doi:10.1097/PRS.0b013e318230c521.
[7] P.V. Peplow, G.D. Baxter, Gene expression and release of growth factors during delayed wound healing: a review of studies in diabetic animals and possible combined laser phototherapy and growth factor treatment to enhance healing, Photomed. Laser Surg. 30 (2012) 617–636, doi:10.1089/pho.2012.3312.
[8] Y. Taniyama, R. Morishita, K. Hiraoka, M. Aoki, H. Nakagami, K. Yamasaki, K. Matsumoto, T. Nakamura, Y. Kaneda, T. Ogihara, Therapeutic angiogenesis induced by human hepatocyte growth gactor gene in rat diabetic hind limb ischemia model, Circulation 104 (2001) 2344–2350, doi:10.1161/hc4401.098470.
[9] N. Smith, J. Overland, J. Greenwood, Local management of deep cavity wounds - current and emerging therapies, Chronic Wound Care Manag. Res. (2015) 159, doi:10.2147/CWCMR.S62553.
[10] J. Timmons, D. Johnstone, Cavity wounds: a juicy topic, Wounds UK 18 (2022) 81–85.
[11] Y. Sun, J. Zhao, L. Zhang, Z. Li, S. Lei, Effectiveness and safety of stem cell therapy for diabetic foot: a meta-analysis update, Stem Cell Res. Ther. 13 (2022) 416, doi:10.1186/s13287-022-03110-9.
[12] L. Jin, X. Wang, Z. Qiao, Y. Deng, The safety and efficacy of mesenchymal stem cell therapy in diabetic lower extremity vascular disease: a meta-analysis and systematic review, Cytotherapy 24 (2022) 225–234, doi:10.1016/j.jcyt.2021.08.001.
[13] J. Guo, A. Dardik, K. Fang, R. Huang, Y. Gu, Meta-analysis on the treatment of diabetic foot ulcers with autologous stem cells, Stem Cell Res. Ther. 8 (2017) 228, doi:10.1186/s13287-017-0683-2.
[14] S. Wangler, A. Kamali, C. Wapp, K. Wuertz-Kozak, S. Häckel, C. Fortes, L.M. Benneker, L. Haglund, R.G. Richards, M. Alini, M. Peroglio, S. Grad, Uncovering the secretome of mesenchymal stromal cells exposed to healthy, traumatic, and degenerative intervertebral discs: a proteomic analysis, Stem Cell Res. Ther. 12 (2021) 11, doi:10.1186/s13287-020-02062-2.
[15] S. Hendrawan, Y. Kusnadi, C.A. Lagonda, D. Fauza, J. Lheman, E. Budi, B.S. Manurung, H.U. Baer, S.T. Tan, Wound healing potential of human umbilical cord mesenchymal stem cell conditioned medium: an *in vitro* and *in vivo* study in diabetes-induced rats, Vet. World. 14 (2021) 2109–2117, doi:10.14202/vetworld.2021.2109-2117.
[16] C.Y. Fong, K. Tam, S. Cheyyatraivendran, S.U. Gan, K. Gauthaman, A. Armugam, K. Jeyaseelan, M. Choolani, A. Biswas, A. Bongso, Human Wharton's jelly stem cells and its conditioned medium enhance healing of excisional and diabetic wounds, J. Cell. Biochem. 115 (2014) 290–302, doi:10.1002/jcb.24661.
[17] S. Hendrawan, E. Bono, A. Hutter, U. Weber, J. Lheman, H.U. Baer, Evaluation of 3D PLLA scaffolds coated with nano-thick collagen as carrier for hepatocytes, J. Biomed. Mater. Res. - Part B Appl. Biomater. 109 (2021) 723–732, doi:10.1002/jbm.b.34738.
[18] H.U. Baer, S. Hendrawan, S. The, S.A. Lelosutan, G. Salim, T. Lindl, S. Mathes, U. Graf-Hausner, U. Weber, R. Watson, B. Sutedja, The intracorporeal autologous hepatocyte matrix implant for the treatment of chronic liver disease: a modified clinical phase I study, World J Surg Surg. Res. 1067 (2018).
[19] S. Hendrawan, J. Lheman, Nuraeni, U. Weber, H.U. Baer, Hepatocyte and islet cell cotransplantation on Poly-L-Lactide matrix for the treatment of liver cirrhosis, Int. J. Hepatol. 2020 (2020) 1–6, doi:10.1155/2020/5410359.
[20] S. Hendrawan, I. Yusuf, M. Hatta, M. Aman, I. Patellongi, A.L. Serra, G. Lawrence, U. Weber, B. Sutedja, H.U. Baer, Allogeneic islet cells implant on poly- l -lactide matrix to reduce hyperglycaemia in streptozotocin-induced diabetic rat, Pancreatology 17 (2017) 411–418, doi:10.1016/j.pan.2017.02.017.
[21] X. Wang, J. Ge, E.E. Tredget, Y. Wu, The mouse excisional wound splinting model, including applications for stem cell transplantation, Nat. Protoc. 8 (2013) 302–309, doi:10.1038/nprot.2013.002.
[22] A.H.A. Al-Rikabi, D.J. Tobin, K. Riches-Suman, M.J. Thornton, Dermal fibroblasts cultured from donors with type 2 diabetes mellitus retain an epigenetic memory associated with poor wound healing responses, Sci. Rep. 11 (2021) 1474, doi:10.1038/s41598-020-80072-z.
[23] H. Pham, R. Tonai, M. Wu, C. Birtolo, M. Chen, CD73, CD90, CD105 and Cadherin-11 RT-PCR screening for mesenchymal stem cells from cryopreserved human cord tissue, Int. J. Stem Cells. 11 (2018) 26–38, doi:10.15283/ijsc17015.
[24] S. Mariya, F.N.A. Dewi, I.H. Suparto, G.K. Wilkerson, J.M. Cline, Permanawati, D. Iskandriati, I.N. Budiarsa, D. Sajuthi, Mammary gland cell culture of Macaca fascicularis as a reservoir for stem cells, HAYATI J. Biosci. 24 (2017) 136–141, doi:10.1016/j.hjb.2017.09.002.
[25] G. Chen, A. Okamura, K. Sugiyama, M.J. Wozniak, N. Kawazoe, S. Sato, T. Tateishi, Surface modification of porous scaffolds with nanothick collagen layer by centrifugation and freeze-drying, J. Biomed. Mater. Res. - Part B Appl. Biomater. 90 B (2009) 864–872, doi:10.1002/jbm.b.31356.
[26] K. Sugiyama, A. Okamura, N. Kawazoe, T. Tateishi, S. Sato, G. Chen, Coating of collagen on a poly(l-lactic acid) sponge surface for tissue engineering, Mater. Sci. Eng. C. 32 (2012) 290–295, doi:10.1016/j.msec.2011.10.031.
[27] C.J. Liao, C.F. Chen, J.H. Chen, S.F. Chiang, Y.J. Lin, K.Y. Chang, Fabrication of porous biodegradable polymer scaffolds using a solvent merging/particulate leaching method, J. Biomed. Mater. Res. 59 (2002) 676–681, doi:10.1002/jbm.10030.
[28] Z. Yang, C. Wang, H. Gao, L. Jia, H. Zeng, L. Zheng, C. Wang, H. Zhang, L. Wang, J. Song, Y. Fan, Biomechanical effects of 3D-printed bioceramic scaffolds with porous gradient structures on the regeneration of alveolar bone defect: a comprehensive study, Front. Bioeng. Biotechnol. 10 (2022) 1–18, doi:10.3389/fbioe.2022.882631.
[29] Q. Zhang, H. Lu, N. Kawazoe, G. Chen, Preparation of collagen scaffolds with controlled pore structures and improved mechanical property for cartilage tissue engineering, J. Bioact. Compat. Polym. 28 (2013) 426–438, doi:10.1177/0883911513494620.
[30] T. Yoshioka, F. Kamada, N. Kawazoe, T. Tateishi, G. Chen, Structural changes and biodegradation of PLLA, PCL, and PLGA sponges during *in vitro* incubation, Polym. Eng. Sci. 50 (2010) 1895–1903, doi:10.1002/pen.21714.
[31] M. Horimizu, T. Kawase, Y. Nakajima, K. Okuda, M. Nagata, L.F. Wolff, H. Yoshie, An improved freeze-dried PRP-coated biodegradable material suitable for connective tissue regenerative therapy, Cryobiology 66 (2013) 223–232, doi:10.1016/j.cryobiol.2013.01.006.
[32] C. Hamilton, A. Callanan, Secreted endothelial cell factors immobilized on collagen scaffolds enhance the recipient endothelial cell environment, Biores. Open Access. 5 (2016) 61–71, doi:10.1089/biores.2016.0003.
[33] C.W. Li, W.T. Pan, J.C. Ju, G.J. Wang, An endothelial cultured condition medium embedded porous PLGA scaffold for the enhancement of mouse embryonic stem cell differentiation, Biomed. Mater. 11 (2016) 25015, doi:10.1088/1748-6041/11/2/025015.
[34] S. Martinotti, E. Ranzato, Scratch Wound Healing Assay, (2019) 225–229, https://doi.org/10.1007/7651_2019_259.
[35] W.N. Arifin, W.M. Zahiruddin, Sample size calculation in animal studies using resource equation approach, Malaysian J. Med. Sci. 24 (2017) 101–105, doi:10.21315/mjms2017.24.5.11.
[36] B.L. Furman, Streptozotocin-induced diabetic models in mice and rats, Curr. Protoc. 1 (2021) 1–21, doi:10.1002/cpz1.78.
[37] S.C. Shin, Y. Seo, H.Y. Park, D.W. Jung, T.H. Shin, H. Son, Y.K. Kim, J.C. Lee, E.S. Sung, J.Y. Jang, H.S. Kim, B.J. Lee, Regenerative potential of tonsil mesenchymal stem cells on surgical cutaneous defect, Cell Death Dis 9 (2018), doi:10.1038/s41419-017-0248-4.
[38] J. Aragón-Sánchez, Y. Quintana-Marrero, C. Aragón-Hernández, M.J. Hernández-Herero, ImageJ: a free, easy, and reliable method to measure leg ulcers using digital pictures, Int. J. Low. Extrem. Wounds. 16 (2017) 269–273, doi:10.1177/1534734617744951.

[39] F. Carfì Pavia, M. Di Bella, V. Brucato, V. Blanda, F. Zummo, I. Vitrano, C. Di Liegro, G. Ghersi, I. Di Liegro, G. Schiera, A 3D-scaffold of PLLA induces the morphological differentiation and migration of primary astrocytes and promotes the production of extracellular vesicles, Mol. Med. Rep. (2019), doi:10.3892/mmr.2019.10351.
[40] N. Rahim, M. Rasidi, Mechanical properties of porous Polylactic Acid (PLA) via salt leaching method, IOP Conf. Ser. Mater. Sci. Eng. 864 (2020) 012124, doi:10.1088/1757-899X/864/1/012124.
[41] L. Gaohua, X. Miao, L. Dou, Crosstalk of physiological pH and chemical pKa under the umbrella of physiologically based pharmacokinetic modeling of drug absorption, distribution, metabolism, excretion, and toxicity, Expert Opin. Drug Metab. Toxicol. 17 (2021) 1103–1124, doi:10.1080/17425255.2021.1951223.
[42] M. Bundó, B. Vlacho, J. Llussà, I. Bobé, M. Aivar, C. Ciria, A. Martínez-Sánchez, J. Real, M. Mata-Cases, X. Cos, M. Dòria, J. Viade, J. Franch-Nadal, D. Mauricio, Prediction of outcomes in subjects with type 2 diabetes and diabetic foot ulcers in Catalonian primary care centers: a multicenter observational study, J. Foot Ankle Res. 16 (8) (2023), doi:10.1186/s13047-023-00602-6.
[43] F. Shams, H. Moravvej, S. Hosseinzadeh, E. Mostafavi, H. Bayat, B. Kazemi, M. Bandehpour, E. Rostami, A. Rahimpour, H. Moosavian, Overexpression of VEGF in dermal fibroblast cells accelerates the angiogenesis and wound healing function: *in vitro* and *in vivo* studies, Sci. Rep. 12 (2022) 18529, doi:10.1038/s41598-022-23304-8.
[44] M.E. Gerritsen, HGF and VEGF: a dynamic duo, Circ. Res. 96 (2005) 272–273, doi:10.1161/01.RES.0000157575.66295.e0.
[45] M. Nakamichi, Y. Akishima-Fukasawa, C. Fujisawa, T. Mikami, K. Onishi, Y. Akasaka, Basic fibroblast growth factor induces angiogenic properties of fibrocytes to stimulate vascular formation during wound healing, Am. J. Pathol. 186 (2016) 3203–3216, doi:10.1016/j.ajpath.2016.08.015.
[46] O. Ørum, M. Hansen, C.H. Jensen, H.A. Sørensen, L.B. Jensen, K. Hørslev-Petersen, B. Teisner, Procollagen type I N-terminal propeptide (PINP) as an indicator of type I collagen metabolism: ELISA development, reference interval, and hypovitaminosis D induced hyperparathyroidism, Bone 19 (1996) 157–163, doi:10.1016/8756-3282(96)00165-2.
[47] Z. Guo, D. Bo, Y. He, X. Luo, H. Li, Degradation properties of chitosan microspheres/poly(L-lactic acid) composite *in vitro* and *in vivo*, Carbohydr. Polym. 193 (2018) 1–8, doi:10.1016/j.carbpol.2018.03.067.
[48] R. Vaid, E. Yildirim, M.A. Pasquinelli, M.W. King, Hydrolytic degradation of Polylactic Acid fibers as a function of pH and exposure time, Molecules 26 (2021) 7554, doi:10.3390/molecules26247554.
[49] A.R. Rosa, D. Steffens, B. Santi, K. Quintiliano, N. Steffen, D.A. Pilger, P. Pranke, Development of VEGF-loaded PLGA matrices in association with mesenchymal stem cells for tissue engineering, Brazilian J. Med. Biol. Res. 50 (2017) 1–12, doi:10.1590/1414-431x20175648.
[50] K. Carter, H.J. Lee, K.S. Na, G.M. Fernandes-Cunha, I.J. Blanco, A. Djalilian, D. Myung, Characterizing the impact of 2D and 3D culture conditions on the therapeutic effects of human mesenchymal stem cell secretome on corneal wound healing *in vitro* and ex vivo, Acta Biomater 99 (2019) 247–257, doi:10.1016/j.actbio.2019.09.022.
[51] R. Edmondson, J.J. Broglie, A.F. Adcock, L. Yang, Three-dimensional cell culture systems and their applications in drug discovery and cell-based biosensors, Assay Drug Dev. Technol. 12 (2014) 207–218, doi:10.1089/adt.2014.573.
[52] H. Haryanto, D. Arisandi, S. Suriadi, I. Imran, K. Ogai, H. Sanada, M. Okuwa, J. Sugama, Relationship between maceration and wound healing on diabetic foot ulcers in Indonesia: a prospective study, Int. Wound J. 14 (2017) 516–522, doi:10.1111/iwj.12638.
[53] E. Everett, N. Mathioudakis, J. Hopkins, Update on management of diabetic foot ulcers, 1411 (2018) 153–165, https://doi.org/10.1111/nyas.13569.
[54] E.N. Lamme, R.T.J. Van Leeuwen, J.R. Mekkes, E. Middelkoop, Allogeneic fibroblasts in dermal substitutes induce inflammation and scar formation, Wound Repair Regen 10 (2002) 152–160, doi:10.1046/j.1524-475X.2002.10901.x.
[55] A. Farrokhi, M. Rahavi, S. Jo, R. Jalili, C.J. Lim, A. Ghahsary, G.S.D. Reid, Inflammatory immune responses trigger rejection of allogeneic fibroblasts transplanted into mouse skin, Cell Transplant 31 (2022) 1–12, doi:10.1177/09636897221113803.
[56] G. Chen, F. Wang, X. Zhang, Y. Shang, Y. Zhao, Living microecological hydrogels for wound healing, Sci. Adv. 9 (2023) 1–9, doi:10.1126/sciadv.adg3478.
[57] X. Wu, D. Huang, Y. Xu, G. Chen, Y. Zhao, Microfluidic templated stem cell spheroid microneedles for diabetic wound treatment, Adv. Mater. 35 (2023) 1–10, doi:10.1002/adma.202301064.
[58] X. Zhang, J. Gan, L. Fan, Z. Luo, Y. Zhao, Bioinspired adaptable indwelling microneedles for treatment of diabetic ulcers, Adv. Mater. 35 (2023) 1–10, doi:10.1002/adma.202210903.